International Journal of Pharmaceutics 430 (2012) 328–334

Contents lists available at SciVerse ScienceDirect

International Journal of Pharmaceutics

journal homepage: www.elsevier.com/locate/ijpharm

Differential efficacy of DOTAP enantiomers for siRNA delivery *in vitro*

Megan Cavanaugh Terp[a,d], Finn Bauer[e], Yasuro Sugimoto[b], Bo Yu[a,d], Robert W. Brueggemeier[b], L. James Lee[a,d,*], Robert J. Lee[c,d,**]

[a] Department of Chemical and Biomolecular Engineering, The Ohio State University, Columbus, OH, USA
[b] Division of Medicinal Chemistry and Pharmacognosy, College of Pharmacy, The Ohio State University, Columbus, OH, USA
[c] Division of Pharmaceutics, College of Pharmacy, The Ohio State University, Columbus, OH, USA
[d] NSF Nanoscale Science and Engineering Center (NSEC) for Affordable Nanoengineering of Polymeric Biomedical Devices, The Ohio State University, Columbus, OH, USA
[e] Drug Delivery Application, EMD Millipore, A Division of Merck KGaA, Woburn, MA, USA

ARTICLE INFO

Article history:
Received 4 October 2011
Received in revised form 27 March 2012
Accepted 3 April 2012
Available online 15 April 2012

Keywords:
DOTAP
Enantiomer
siRNA
Lipoplex
Aromatase
Modeling

ABSTRACT

DOTAP, as a racemic mixture, is a cationic lipid and a widely used transfection reagent. In this study, the effect of DOTAP's stereochemical structure on transfection efficiency was evaluated *in vitro*. Racemic and enantiomerically pure DOTAP were used in lipoplex formulations to deliver siRNA to MCF-7 cells, targeting the aromatase enzyme. At the 50 nM siRNA concentration and lipid-to-RNA charge ratios of 4 and 5, the R enantiomer of DOTAP was found to perform better than either the S- or the racemic agent. In addition, at 10 nM siRNA concentration and a charge ratio of 3, the R- lipoplex formulation silenced aromatase by ~50% whereas the S and racemic formulations caused no significant target downregulation. Differences in lipid packing were modeled using membrane simulations. The results showed that, when combined with cholesterol, pure R-DOTAP and S-DOTAP enantiomers had 105% and 115% of lipid density relative to racemic DOTAP, respectively. These findings suggest an important role of lipid chirality in future development of lipid based siRNA delivery systems.

1. Introduction

Cationic lipids have successfully been used as transfection reagents since the introduction of 1,2-di-O-octadecenyl-3-trimethylammonium propane (DOTMA) by Felgner et al. (1987). Today, one of the most widely used cationic lipids is 1,2-dioleoyl-3-trimethylammonium-propane (DOTAP) due to its high transfection efficiency and low toxicity (Stamatatos et al., 1988; Simberg et al., 2004). The DOTAP products reported in the literature contain a racemic mixture of DOTAP's enantiomers, R and S, which are non-superimposable mirror images, as shown in Fig. 1. Each of a DOTAP molecule's two 18-carbon acyl chains contains an unsaturated double bond in the cis configuration, causing kinks in the hydrocarbon chains. This, in turn, can impact the packing behavior of the lipid bilayer. In fact, the racemic mixture of DOTAP has a phase transition temperature that is 5 °C lower than either of the pure enantiomers, R- or S- (Platscher and Hedinger, 2008), suggesting that enantiomerically pure molecules of DOTAP can pack more tightly than the racemic mixture. Furthermore, R-DOTAP appears to have a phase transition temperature that is 0.5 °C lower than the S-DOTAP enantiomer. It is possible that one of these enantiomers organizes at a density that is favorable for siRNA delivery. Hence, a lipid bilayer composed of the racemic mixture of DOTAP likely has a less dense packing structure than one containing the enantiomerically pure DOTAP and the lipid packing could also be different amongst the pure enantiomers. Whether the stereochemical structure of cationic lipid molecules affects transfection efficiency has not been fully explored (Vasievich et al., 2011). It is possible that enantiomeric preferences exist with cationic lipids for delivery of nucleic acids to cells.

Breast cancer is the most common cancer among women in the US. Aromatase is required for the production of estrogen, which in turn is frequently required for sustaining breast cancer growth (Deroo and Korach, 2006). Aromatase inhibitors (AIs) are currently the standard treatment for estrogen dependent, postmenopausal breast cancer patients. However, AI use is associated with side effects, such as unbearable musculoskeletal pain or osteoporosis (Janni and Hepp, 2010; Wang et al., 2011). By strategically delivering siRNA that silences aromatase using a liposomal system targeting the tumor, these side effects may be reduced or eliminated. However, an effective delivery method is required for such treatment to be developed clinically. This study investigates the effect of stereochemistry of DOTAP on delivery of siRNA, using aromatase and MCF-7 breast cancer cells as an *in vitro* model.

* Corresponding author at: Department of Chemical and Biomolecular Engineering, 1012 Smith Lab, 174 West 18th Ave, Columbus, OH 43210, USA. Tel.: +1 614 292 2408; fax: +1 614 292 3769.
** Corresponding author at: College of Pharmacy, 500 West 12th Ave, Columbus, OH 43210, USA. Tel.: +1 614 292 4172; fax: +1 614 292 7766.
E-mail addresses: lee.31@osu.edu (L.J. Lee), lee.1339@osu.edu (R.J. Lee).

0378-5173/$ – see front matter © 2012 Elsevier B.V. All rights reserved.
http://dx.doi.org/10.1016/j.ijpharm.2012.04.017

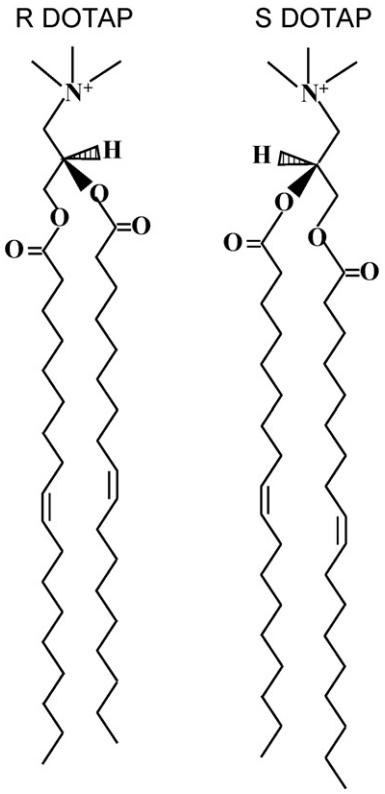

Fig. 1. Stereochemical renderings of R- and S-DOTAP molecules.

2. Materials and methods

2.1. Materials

The R, S, and racemic DOTAP chloride enantiomers were kindly provided by Merck KGaA (Darmstadt, Germany). Cholesterol was purchased from Sigma–Aldrich (St. Louis, MO). Stealth siRNA targeting the open reading frame of aromatase (siAROM) and non-targeting control siRNA (siCTRL) were purchased from Invitrogen (Carlsbad, CA). The passenger sequence for siAROM from 5′–3′ is CGGUAUGCAUGAGAAAGGCAUCAUA and the guide sequence is UAUGAUGCCUUUCUCAUGCAUACCG. For siCTRL, the sequences are (5′–3′) CGGGUACGUGAAAGACGUACAUAUA and UAUAUGUACGUCUUUCACGUACCCG. Radiolabeled [1β-^{3}H]androst-4-ene-3,17-dione (SA: 0.973 TBq/mmol) was purchased from NEN Life Science Products (Boston, MA). Aromatase inhibitor 7α-(4′-amino) phenylthio-1,4-androstaediene-3,17-dione (7α-APTADD) was synthesized following published methods (Brueggemeier et al., 1987).

2.2. Lipoplex preparation

Cholesterol was dissolved in warm ethanol at 5 mg/ml and DOTAP enantiomers were dissolved in ethanol at 50 mg/ml. These solutions were mixed at DOTAP:cholesterol 1:1 mol/mol and total lipid concentration of 10 mg/ml. Liposomes were prepared by the ethanol injection method (Batzri and Korn, 1973). Briefly, 100 μl of the lipid/ethanol solution was drawn into a syringe and injected into 900 μl of PBS buffer while vortexing, forming liposomes that were then bath sonicated for 5 min. Lipoplexes were formed by adding an equal volume of siRNA to the liposomes, each solution diluted to the appropriate concentrations to provide the desired charge ratio and total siRNA concentration for the formulation being tested. Finally, 2× volume of OptiMEM culture media (Invitrogen) was added to the lipoplex mixture, which amounted to 100 μl lipoplex plus 200 μl media (total of 300 μl lipoplex mixture) being added per well. Charge ratios (+/−) were calculated by assuming one positive charge per DOTAP molecule and 50 negative charges per siRNA molecule (1 negative charge per nucleotide).

2.3. Cell culture and transfection methods

MCF-7 cells were stably transfected with the human aromatase linked to neomycin resistance gene. MCF-7 cells (ATCC, Manassas, VA) in an exponential growth phase were plated without antibiotics into 6-well plates. These cells were transfected with pcDNA6-human-aromatase when they reached 90% confluency. The transfection was performed according to the supplier instructions using Lipofectamine 2000 (Invitrogen). After 48 h, the cells were transferred to selective media containing G418 sulfate (800 μg/ml). Then the aromatase-positive cells were subcloned into a 24-well plate by a cloning cylinder (Bellco, Vineland, NJ) and an individual cell clone that was aromatase activity positive was propagated and designated MCF-7-pcDNA-arom. Individual clones were maintained in a culture medium containing G418 sulfate (200 μg/ml).

MCF-7-pcDNA-arom cells were grown at 37 °C, 5% CO_2 as a monolayer in complete media containing 5% FBS and 0.04% gentamycin. Three days before transfection, 5×10^4 cells were seeded in 2 ml of growth medium in 6 well plates. For transfection, the media was removed and replaced with 700 μl of OptiMEM media and then 300 μl of the lipoplex mixture was added for a total volume of 1 ml. After 6 h, the transfection was halted through dilution by adding 3 ml of complete media and the cells were incubated for 48 h before the tritiated water release assay was performed.

2.4. Tritiated water release assay to measure aromatase activity

Aromatase activity was measured using the tritium water-release assay, as described previously (Zheng et al., 2010). This assay measures the amount of [^{3}H]H_2O released during the conversion of the substrate [1β-^{3}H]androst-4-ene-3,17-dione into estrone by aromatase. Briefly, 48 h after the lipoplexes were administered, fresh culture media containing 1 μCi [1β-^{3}H]androstenedione was added to the cells and allowed to incubate for 2 h. Steroids in the media were removed using diethyl ether extraction; that is, ether was added to the media, vortexed and centrifuged. The organic phase was then separated from the aqueous phase by freezing the aqueous phase in a dry ice/ethanol bath after centrifugation and then removing the unfrozen ether supernatant by vacuum suction. The ether extraction process was repeated three times. The aqueous phase was further purified by adding 200 μl of 1% charcoal/0.5% dextran solution and incubated for 10 min at 42 °C to remove any remaining steroids. Finally, the charcoal/aqueous phase mixture was centrifuged and a 600 μl aliquot of the supernatant was added to scintillation cocktail in a 5 ml scintillation vial and counted for radioactivity. The amount of radioactivity in the [^{3}H]H_2O was normalized with the total DNA content. Cells were lyzed with 980 μl of 8 mM NaOH, incubated at 60 °C for 10 min, and the solution was then neutralized with 20 μl of 1 M HEPES. The DNA content was measured on a Tecan GENios reader (Tecan Systems, Inc., CA, USA) by taking a 100 μl aliquot and adding HOECHST 33258 fluorescent dye, using a known amount of calf thymus DNA as the standard. The excitation and emission wavelengths used were 360 and 465 nm, respectively. In addition, a chemical aromatase inhibitor (7α-APTADD, 100 nM) served as the baseline reference for non-specific exchanges of the radioactive 1β-^{3}H with water, assuming 100% inhibition. Each variable was performed in triplicate except for the untreated controls, which had 6 replicates.

The results were statistically analyzed with one-way ANOVA on GraphPad Prism.

2.5. MTS assay

MCF-7 cells were seeded 2.5 days before transfection in a 96-well plate at a density of 2500 cells per well. Cell viability was measured 48 h after lipoplex administration by removing the culture media and adding MTS [3-(4,5-dimethylthiazol-2-yl)-5-(3-carboxymethoxyphenyl)-2-(4-sulfophenyl)-2H-tetrazolium], in the presence of phenazine methosulfate (PMS). After 2 h incubation at 37 °C, the plates were read at OD 490 nm to detect the formazan product after MTS conversion on a Spectra MAX 340 plate reader (Molecular Devices Corp., Sunnyvale, CA, USA). Each variable had 6 replicates.

2.6. CryoTEM

Lipoplex samples were prepared for cryoTEM imaging in a controlled environment vitrification system (CEVS) at 25 °C and 100% relative humidity and then plunged into liquid ethane at its freezing point, as described previously (Bellare et al., 1988; Danino et al., 2001). Imaging of the vitrified samples was performed at 120 kV on an FEI Tecnai T12 G2 TEM with a Gatan 626 cryo-holder system that was maintained at less than −178 °C. Images were captured with a Gatan US1000 high resolution camera and Digital Micrograph software in low dose imaging mode to reduce the amount of radiation damage.

2.7. Membrane modeling

Membranes were modeled on a shape-based algorithm with CELLmicrocosmos 2.2.1 MembraneEditor (Sommer et al., 2011). Membrane patches were designed as double layer stacks of 100 Å × 100 Å. 3D lipid structures of cholesterol were chosen from the MembraneEditor built-in lipid library and DOTAP structures were obtained as described previously (Lonez et al., 2010). Identical lipid compositions were defined for the outer membrane (OM) and inner membrane (IM) to 50% cholesterol combined with 50% R-DOTAP (pure R enantiomer), 50% S-DOTAP (pure S enantiomer) or 25% R- and 25% S-DOTAP (racemic mixture), respectively. A simulated annealing protocol was followed as suggested in Sommer et al. allowing for additional lipids to be placed into the membrane patch during the simulation. Three random seeds were selected as starting points for the simulation of R-, S-, and racemic DOTAP cholesterol membranes, respectively. Lipid density was evaluated based on the total number of lipids per patch.

2.8. Confocal microscopy to measure cellular uptake pathway

Confocal microscopy was used to determine whether different cellular uptake pathways are utilized by the DOTAP enantiomers. Samples were prepared by seeding 1×10^4 cells in 500 ml of growth medium in 24 well plates on top of pre-sterilized round glass coverslips. Two days after seeding, the growth media was removed and lipoplexes containing Cy3-siRNA were administered in Optimem media along with one of the three common endocytic pathway markers that were also fluorescently labeled; either transferrin-AlexaFluor 488 (20 μg, Invitrogen), which is internalized via clathrin-mediated endocytosis (Hopkins and Trowbridge, 1983), 70 kDa dextran-FITC (0.6 μg, Sigma–Aldrich), associated with macropinocytosis (Oliver et al., 1984), or cholera toxin subunit B-AlexaFluor 488 (CT-B, 1 μg, Invitrogen), which can be used to identify lipid raft/caveolae mediated endocytosis (Orlandi and Fishman, 1998; Nichols et al., 2001). After 1.5 h, the media was removed and the cells were gently washed twice with PBS and then fixed with 200 μl of 4% paraformaldehyde for 20 min. Finally, the round glass coverslips were carefully removed and rinsed once more with PBS before being mounted on a glass slide for observation. The samples were observed by an Olympus FV1000 Filter Confocal Microscope (Olympus Optical Co., Tokyo, Japan) at the appropriate wavelengths. Co-localization of the Cy3-siRNA

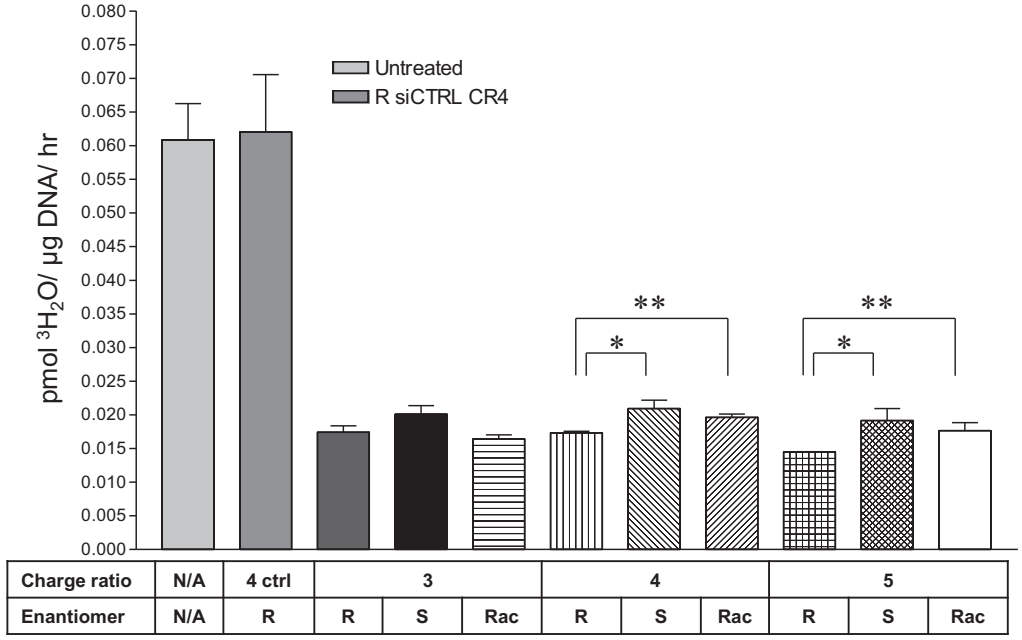

Fig. 2. Effect of charge ratio on transfection efficiency of DOTAP enantiomers. Efficacy measured by relative aromatase activity at varying +/− charge ratios (CR = 3, 4 and 5) and constant siRNA concentration (50 nM). Formulations consist of 1:1 molar ratio of DOTAP:cholesterol using either the R, S, or racemic (Rac) DOTAP enantiomer. Statistically significant differences are as shown with $^*p < 0.01$ and $^{**}p < 0.05$. Each lipoplex variable is also statistically different ($p < 0.001$) from both the untreated control and random siRNA control (siCTRL).

(red) and the applied endocytic marker (green) appeared yellow, which indicated the extent to which the lipoplex particles were internalized by that pathway. Nikon Instruments "Elements" software was then used to determine the Pearson's correlation coefficient (PCC), a reliable parameter that can quantify the degree of overlap between fluorophores for each image (Adler and Parmryd, 2010). The PCCs of the R-, S-, and racemic DOTAP variables at each condition were statistically analyzed with one-way ANOVA on GraphPad Prism. At least 15 separate images per enantiomer per condition were visually analyzed and at least 8 images per condition were analyzed for PCC.

3. Results

3.1. Downregulation of aromatase enzyme after lipoplex administration

The effect of the stereochemical structure of the cationic lipid DOTAP on siRNA delivery efficiency was measured in MCF-7 cells. The siRNA targeted the aromatase enzyme (siAROM) and the extent of gene silencing was measured by comparing the aromatase activity of each formulation to an untreated control, which was defined as having 100% aromatase activity. All liposome formulations consisted of a 1:1 molar ratio of DOTAP enantiomer (or racemic mixture) to cholesterol. Fig. 2 shows the effect of DOTAP enantiomers at a constant siRNA concentration of 50 nM but at varying charge ratios (CR) of +/− = 3, 4, and 5. At 50 nM, all siAROM lipoplex formulations resulted in significant downregulation of aromatase. At 50 nM and CR = 4 and CR = 5, the R- enantiomer was more effective than both S and racemic but the differences between the means were only 6–8% and 4–5%, respectively.

Fig. 3 compares the DOTAP enantiomers at a constant CR of 3 but at varying siRNA concentration (10, 25, and 50 nM). While no significant differences between the enantiomers or racemic were found at 25 or 50 nM, a large difference was found at 10 nM. Here the R- formulation was found to be twice as effective and silenced aromatase by 47% whereas the S- and racemic showed little to no down-regulation.

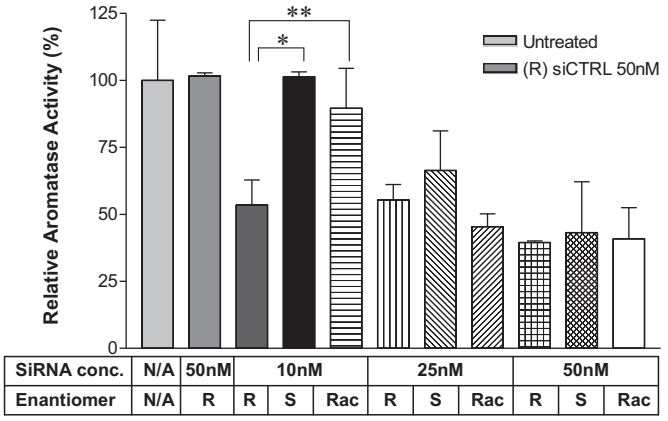

Fig. 3. Effect of siRNA concentration on transfection efficiency of DOTAP enantiomers. Relative aromatase activity was determined at varying siRNA concentrations (10, 25 and 50 nM) and constant +/− charge ratio of 3. Statistical differences are as shown with $^{*}p < 0.01$ and $^{**}p < 0.05$. All lipoplex variables were also statistically different (at least $p < 0.05$) from both the untreated control and the random siRNA control (siCTRL) except for S10 and racemic 10, which were not statistically different than either control.

3.2. Membrane modeling

Differences in lipid packing were evaluated by membrane modeling. Membranes were modeled as 1:1 DOTAP:cholesterol with either the pure R-DOTAP, pure S-DOTAP enantiomers or a racemic mixture of DOTAP. Three simulations of racemic DOTAP resulted in an average of 565.0 ± 4.6 lipids per given membrane size, which was defined as 100% lipid density. Simulations of pure R-DOTAP and pure S-DOTAP enantiomers instead of the racemic mixture resulted in 590.7 ± 2.5 and 649.0 ± 22.6 lipids, respectively, which translates to 105% and 115% of lipid density relative to racemic DOTAP. Despite the large variation of the results for the S-DOTAP:cholesterol, statistical difference ($p < 0.05$) was found for racemic *vs.* R and racemic *vs.* S. Meanwhile, there was no statistical difference between R and S enantiomers (Fig. 4).

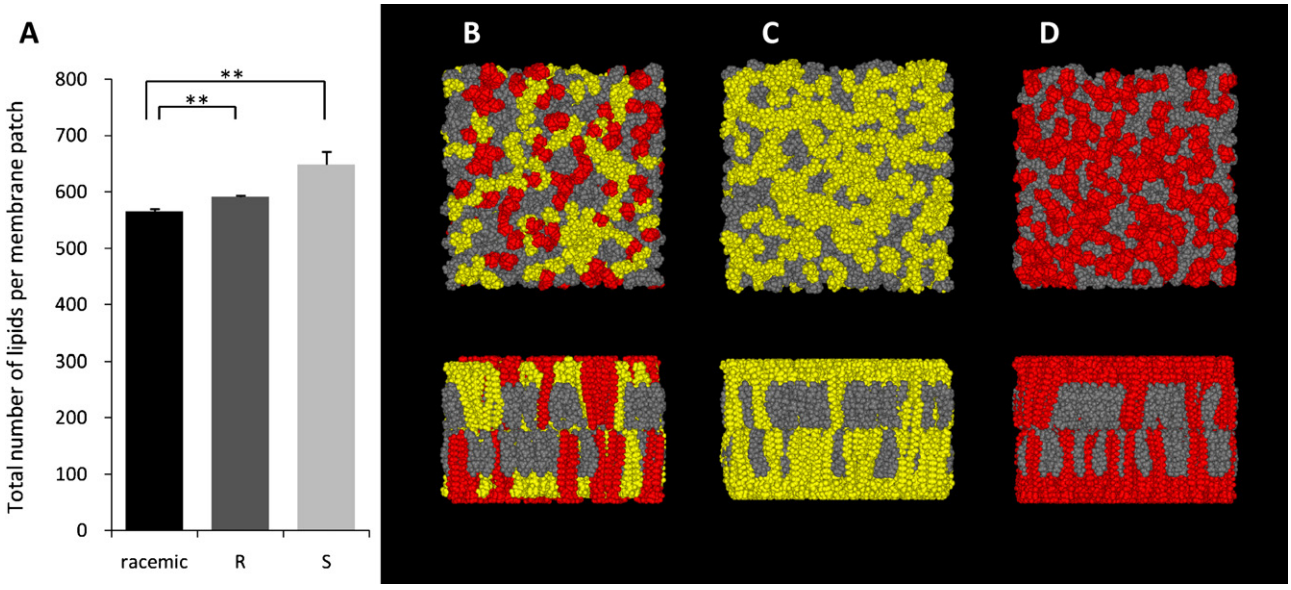

Fig. 4. Membrane modeling of 1:1 DOTAP:cholesterol. Total number of lipids per 100 Å × 100 Å simulated membrane patch (A) of formulations containing 1:1 DOTAP:cholesterol where the racemate represents a 50/50 R- and S-DOTAP mixture, R represents pure R-DOTAP enantiomer and S represents pure S-DOTAP enantiomer. Top view and side view of simulated membrane patches containing cholesterol and racemic DOTAP (B), pure R-DOTAP enantiomer (C), or pure S-DOTAP enantiomer (D); R-DOTAP (yellow), S-DOTAP (red) and cholesterol (gray), atoms are represented as spheres of van-der-Waals radius. Statistical differences are as shown with $^{**}p < 0.05$; $n = 3$. (For interpretation of the references to color in this figure legend, the reader is referred to the web version of the article.)

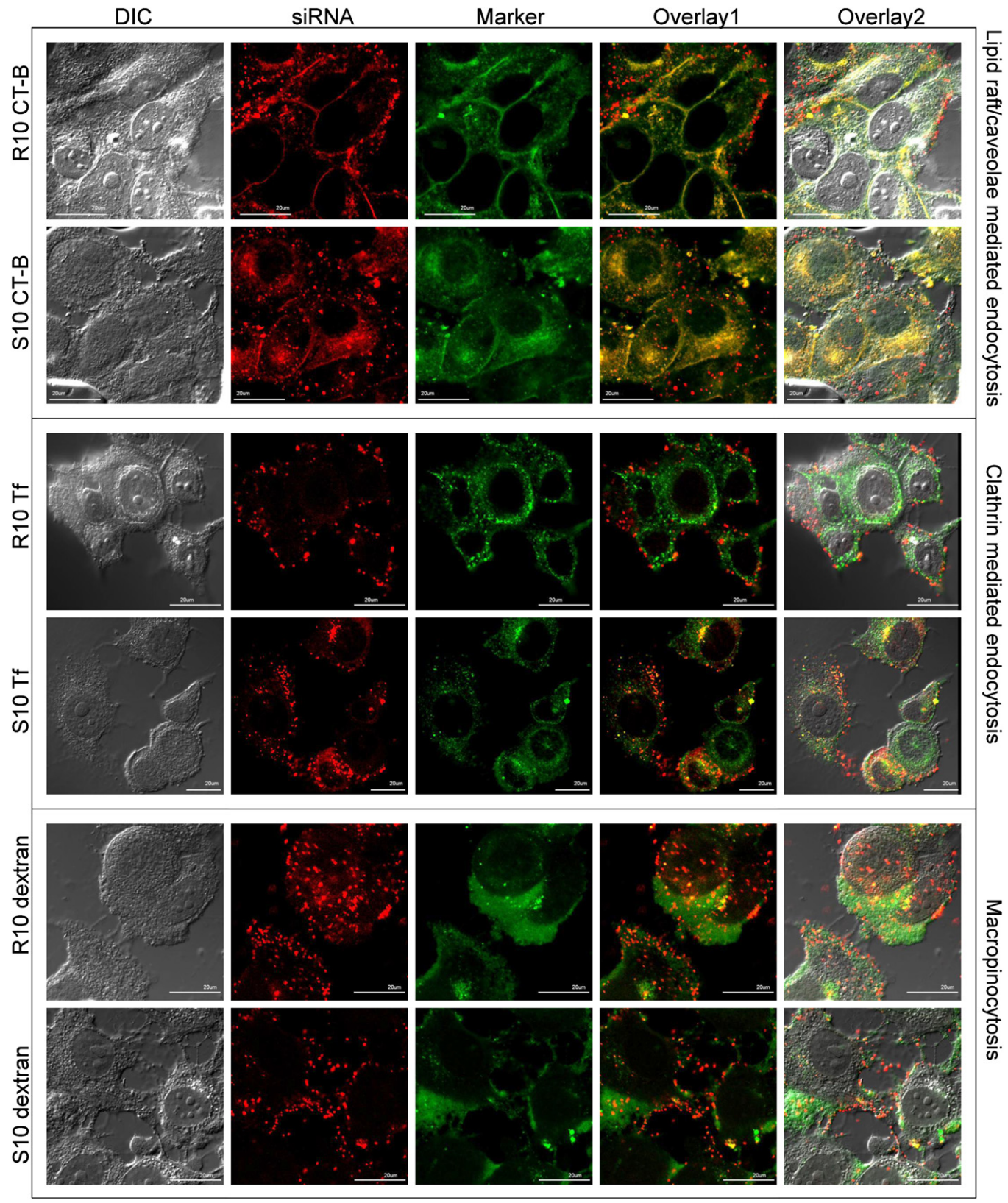

Fig. 5. Endocytosis pathways of R- and S-DOTAP lipoplexes. Confocal images of MCF-7 cells treated with various fluorescently labeled endocytotic markers (green) and R- or S-DOTAP/cholesterol lipoplexes containing Cy3-siRNA (red), conc. 10 nM. Co-localization appears as yellow. (For interpretation of the references to color in this figure legend, the reader is referred to the web version of the article.)

siRNA conc.	Internalization route	DOTAP enantiomer	PCC	
10 nM	Lipid raft/ caveolae mediated	R	0.87 ± 0.04	
		S	0.87 ± 0.03	
		Racemic	0.92 ± 0.06	
	Clathrin mediated endocytosis	R	0.31 ± 0.09	*
		S	0.50 ± 0.07	*
		Racemic	0.54 ± 0.06	*
	Macro-pinocytosis	R	0.47 ± 0.04	
		S	0.43 ± 0.12	
		Racemic	N/A	
25 nM	Lipid raft/ caveolae mediated	R	0.90 ± 0.05	
		S	0.93 ± 0.02	
		Racemic	0.94 ± 0.04	
	Clathrin mediated endocytosis	R	0.58 ± 0.06	
		S	0.66 ± 0.08	
		Racemic	0.64 ± 0.04	
	Macro-pinocytosis	R	0.70 ± 0.06	
		S	0.69 ± 0.08	
		Racemic	0.63 ± 0.07	

Fig. 6. Extent of colocalization of fluorescently labeled lipoplexes and endocytic markers. Pearson correlation coefficients (PCC) indicating co-occurrence of fluorophores in confocal images of MCF-7 cells treated with Cy3-siRNA containing DOTAP/cholesterol lipoplexes at 10 nM or 25 nM and fluorescently labeled endocytic markers. $^{*}p < 0.001$; $n \geq 8$.

3.3. Mechanism of cellular uptake

Confocal microscopy was used to analyze the pathways by which DOTAP based lipoplexes are internalized by MCF-7 cells at a siRNA dosage of 10 nM and 25 nM. Co-localization of fluorescently labeled siRNA and endocytic markers (visible as yellow in the overlaid images) indicated whether the particles were internalized via clathrin mediated endocytosis (Tf), macropinocytosis (dextran70), or lipid raft/caveolae mediated endocytosis (CT-B). Images shown in Fig. 5 are representative of the entire area that was viewed for each condition. There was a very high degree of co-localization on samples treated with CT-B-AlexaFluor488 (PCCs are close to 1) as shown in Fig. 6, indicating that lipid raft/caveolae endocytosis was the primary internalization pathway for lipoplexes for R-, S-, and racemic DOTAP formulations and there were no statistical differences between the three Pearson correlation coefficients at either 10 nM or 25 nM. Lower levels of co-localization were found on samples treated with the Cy3-siRNA and dextran70-FITC indicating lipoplexes were still internalized via macropinocytosis, but less than that of lipid raft/caveolae mediated endocytosis. Interestingly, clathrin mediated endocytosis was not a major internalization pathway. However there was a statistically significant increase ($p < 0.001$) in the PCCs of samples treated with lipoplexes formulated with the S enantiomer and racemic DOTAP *vs.* the R enantiomer at 10 nM. The variation in the extent of co-localization of the Cy3-siRNA and Tf-AlexaFluor488 at 10 nM suggests that S- and racemic DOTAP lipoplexes are internalized to a larger extent by clathrin mediated endocytosis than R-DOTAP lipoplexes are. This difference was not evident at 25 nM.

3.4. Cell viability

Cytotoxicity of the lipoplex formulations was tested on MCF-7 cells at varying siRNA concentrations and constant +/− CR of 3. None of the DOTAP:cholesterol formulations showed decreased cell viability at 48 h after transfection, as shown in Fig. 7.

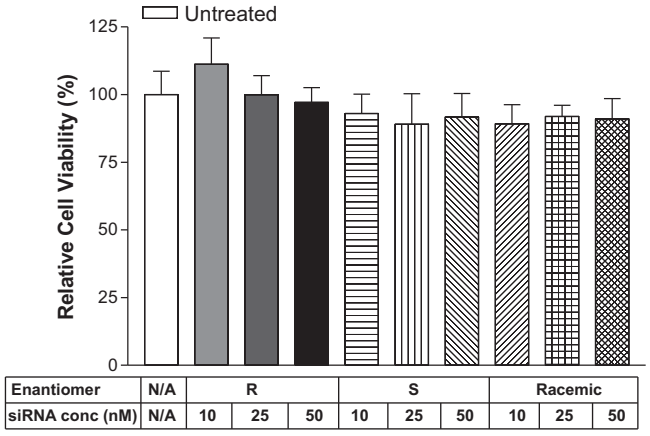

Fig. 7. Cell viability after DOTAP lipoplex treatment. Cell viability was determined by MTS assay 48 h after lipoplex administration at varying siRNA concentrations. Each formulation contains the R, S, or racemic DOTAP at a 1:1 molar ratio with cholesterol and with CR = 3. No significant differences were found between the various formulations and the untreated control ($p > 0.05$) using Dunnet's multiple comparison test.

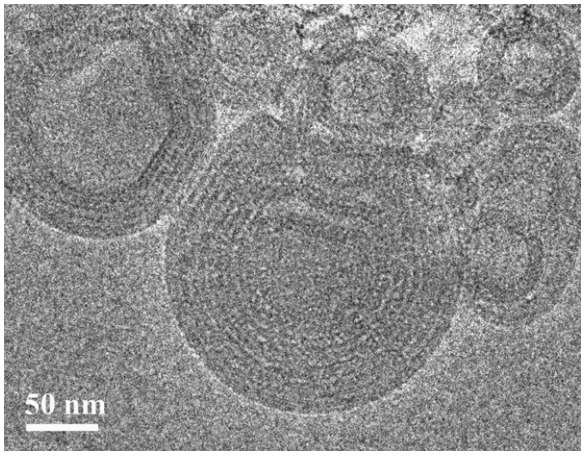

Fig. 8. CryoTEM image of 1:1 racemic DOTAP/cholesterol lipoplex.

3.5. Lipoplex structure by cryoTEM

While the orientation of the DOTAP molecules or the lipid packing cannot be resolved by cryoTEM, the overall structure of the lipoplex particles was observed with this method. The multilamellar structure that is typical of siRNA containing lipoplexes (Desigaux et al., 2007) was visible as shown in Fig. 8, with siRNA molecules packed between the lipid bilayers of racemic DOTAP. The R and S enantiomer formulations were also observed and they exhibited the same onion-like particle structure (data not shown).

4. Discussion and conclusion

Chiral preferences for DOTAP in transfection activity are investigated in this study. A highly relevant question is whether the R enantiomer of DOTAP is better than the racemic mixture, which is the form of DOTAP widely used in the literature. Our modeling data clearly indicate a physical difference among DOTAP:cholesterol membranes when DOTAP is simulated as a racemic mixture *vs.* pure R or pure S enantiomers. Although no statistical difference was observed between the models of pure R- and pure S-DOTAP:cholesterol membranes (the *p* value was just above the

statistical significance at $p = 0.0561$), the published phase transition data points to a small difference between the enantiomers (Platscher and Hedinger, 2008). Regardless, our data indicate that the elimination of one enantiomer of DOTAP can lead to tighter lipid packing and higher lipid densities. In addition, a preference exists in MCF-7 cells for the R enantiomer of DOTAP when used as delivery agent for a siRNA against aromatase. The R enantiomer was found to be statistically better than both S and racemic at higher charge ratios (CR = 4 and 5), but the differences between the means of R *vs.* S and R *vs.* racemic were rather small, *i.e.* less than 10% at 50 nM. However, at a low siRNA concentration of 10 nM and CR = 3, the improved performance of the R enantiomer was much greater. Under these conditions, the R-DOTAP lipoplex formulation silenced aromatase by almost 50% while the S and racemic formulations showed little to no down-regulation. Furthermore, it is not surprising that the superior efficacy of the R enantiomer was not apparent at the higher siRNA concentrations since racemic DOTAP is already a very effective transfection reagent. In fact, near complete aromatase inhibition was found at higher concentrations for all DOTAP formulations (*e.g.* CR = 3 and 100 nM, data not shown). Nevertheless, positively charged particles attract serum proteins and can cause toxicity so the ability to lower the total charge of the lipoplex while maintaining efficacy is important for *in vivo* applications of DOTAP vectors. Even at higher charge ratios, an improvement of 5–10% could be significant in certain applications. Furthermore, since the cost of siRNA is high, any way to reduce the necessary concentration by using a chiral lipid with superior performance could help propel these types of treatment options forward.

Most of the lipoplex formulations containing DOTAP in these studies were able to significantly downregulate aromatase in MCF-7 cells without significant cytotoxicity, as shown by the cell viability results. In these studies, the R enantiomer at 50 nM, CR = 5 resulted in the highest aromatase silencing of 80% and at the lowest siRNA concentration tested 10 nM, the R enantiomer had silencing of 50% while the S and racemic formulations provided no downregulation.

Based on confocal data, the primary internalization pathway was lipid raft/caveolae endocytosis for the DOTAP lipoplexes regardless of enantiomer used as evidenced by the high degree of colocalization. S- and racemic DOTAP lipoplexes had a higher occurrence of clathrin mediated endocytosis than the R-DOTAP lipoplexes at 10 nM. It is possible that the higher degree of clathrin mediated endocytosis by the S- and racemic DOTAP lipoplexes caused a decreased transfection efficiency relative to the R-DOTAP, especially in light of the extensive review of lipoplex endocytosis conducted by Lu et al. (2009) where they found that functional siRNA was not delivered through the clathrin mediated pathway. Therefore if a lower amount of siRNA from the R-DOTAP lipoplexes is degraded in the lysosomes during clathrin mediated endocytosis at 10 nM and is instead internalized through alternative routes, this would result in higher transfection efficiency, as was seen in these studies.

It has been shown that DOTAP in combination with cholesterol is an effective siRNA transfection reagent for MCF-7 cells. Using a liposomal vector to deliver siRNA against aromatase in breast cancer cells is a novel approach to treating estrogen dependent breast cancer. Given the promising *in vitro* data showing a potential role of stereochemistry in transfection, further *in vivo* studies on the DOTAP isomers are warranted.

Acknowledgements

This work was supported in part by NSF grants DGE0221678, EEC-0425626, EEC-0914790, and EEC-0425626 to L. James Lee and DOD grant W81XWH-08-1-0610 to Robert J. Lee. The authors thank Yeshayahu Talmon, Sharon Golan, Ellina Kesselman and Judith Schmidt at the Technion – Israel Institute of Technology for their TEM training and Yun Wu for her assistance on confocal sample preparation.

References

Adler, J., Parmryd, I., 2010. Quantifying colocalization by correlation: the Pearson correlation coefficient is superior to the Mander's overlap coefficient. Cytometry A 77, 733–742.

Batzri, S., Korn, E.D., 1973. Single bilayer liposomes prepared without sonication. Biochim. Biophys. Acta 298, 1015–1019.

Bellare, J.R., Davis, H.T., Scriven, L.E., Talmon, Y., 1988. Controlled environment vitrification system: an improved sample preparation technique. J. Electron Microsc. Tech. 10, 87–111.

Brueggemeier, R.W., Pui-Kai, L., Snider, C.E., Darby, M.V., Katlic, N.E., 1987. 7α alpha-substituted androstenediones as effective in vitro and in vivo inhibitors of aromatase. Steroids 50, 163–178.

Danino, D., Bernheim-Groswasser, A., Talmon, Y., 2001. Digital cryogenic transmission electron microscopy: an advanced tool for direct imaging of complex fluids. Colloid Surf. A 183, 113–122.

Deroo, B.J., Korach, K.S., 2006. Estrogen receptors and human disease. J. Clin. Invest. 3, 561–570.

Desigaux, L., Sainlos, M., Lambert, O., Chevre, R., Letrou-Bonneval, E., Vigneron, J.P., Lehn, P., Lehn, J.M., Pitar, B., 2007. Self-assembled lamellar complexes of siRNA with lipidic aminoglycoside derivatives promote efficient siRNA delivery and interference. Proc. Natl. Acad. Sci. U.S.A. 42, 16534–16539.

Felgner, P.L., Gadek, T.R., Holm, M., Roman, R., Chan, H.W., Wenz, M., Northrop, J.P., Ringold, G.M., Danielson, M., 1987. Lipofection: a highly efficient, lipid-mediated DNA-transfection procedure. Proc. Natl. Acad. Sci. U.S.A. 84, 7413–7417.

Hopkins, C.R., Trowbridge, I.S., 1983. Internalization and processing of transferrin and the transferrin receptor in human carcinoma A431 cells. J. Cell Biol. 97, 508–521.

Janni, W., Hepp, P., 2010. Adjuvant aromatase inhibitor therapy: outcomes and safety. Cancer Treat. Rev. 36, 249–261.

Lonez, C., Lensink, M.F., Kleiren, E., Vanderwinden, J.M., Ruysschaert, J.M., Vandenbranden, M., 2010. Fusogenic activity of cationic lipids and lipid shape distribution. Cell. Mol. Life Sci. 67, 483–494.

Lu, J.L., Langer, R., Chen, J., 2009. A novel mechanism is involved in cationic lipid-mediated functional siRNA delivery. Mol. Pharm. 6, 763–771.

Nichols, B.J., Kenworthy, A.K., Polishchuk, R.S., Lodge, R., Roberts, T.H., Hirschberg, K., Phair, R.D., Lipincott-Schwartz, J., 2001. Rapid cycling of lipid raft markers between the cell surface and Golgi complex. J. Cell Biol. 153, 529–541.

Oliver, J.M., Berlin, R.D., Davis, B.H., 1984. Use of horseradish peroxidase and fluorescent dextrans to study fluid pinocytosis in leukocytes. Methods Enzymol. 108, 336–347.

Orlandi, P.A., Fishman, P.H., 1998. Filipin-dependent inhibition of cholera toxin: evidence for toxin internalization and activation through caveolae-like domains. J. Cell Biol. 141, 905–915.

Platscher, M., Hedinger, A. (inventors), 2008, January 17. Stable crystal modifications of DOTAP chloride. U.S. Patent Application Publication 2008/0014254.

Simberg, D., Weisman, S., Talmon, Y., Barenholz, Y., 2004. DOTAP (and other cationic lipids): chemistry, biophysics, and transfection. Crit. Rev. Ther. Drug 4, 257–317.

Sommer, B., Dingersen, T., Gamroth, C., Schneider, S.E., Rubert, S., Krüger, J., Dietz, K.J., 2011. CELLmicrocosmos 2.2 MembraneEditor: a modular interactive shape-based software approach to solve heterogeneous membrane packing problems. J. Chem. Inf. Model. 51, 1165–1182.

Stamatatos, L., Leventis, R., Zuckermann, M.J., Silvius, J.R., 1988. Interactions of cationic lipid vesicles with negatively charged phospholipid vesicles and biological membranes. Biochemistry 27, 3917–3925.

Vasievich, E.A., Chen, W., Huang, L., 2011. Enantiospecific adjuvant activity of cationic lipid DOTAP in cancer vaccine. Cancer Immunol. Immunother. 5, 629–638.

Wang, L., McLeod, H.L., Weinshilboum, R.M., 2011. Genomics and drug response. N. Engl. J. Med. 364, 1144–1153.

Zheng, Y., Yu, B., Weecharangsan, W., Piao, L., Darby, M., Mao, Y., Koynova, R., Yang, X., Li, H., Xu, S., Lee, L.J., Sugimoto, Y., Brueggemeier, R.W., Lee, R.J., 2010. Transferrin-conjugated lipid-coated PLGA nanoparticles for targeted delivery of aromatase inhibitor 7αAPTADD to breast cancer cells. Int. J. Pharm. 390, 234–241.